B21
ARPA-E-39

Division of Engineering
BROWN UNIVERSITY
PROVIDENCE, R. I.

A PATH INDEPENDENT INTEGRAL AND THE APPROXIMATE ANALYSIS OF STRAIN CONCENTRATION BY NOTCHES AND CRACKS

J. R. RICE

AD653716

Department of Defense
Advanced Research Projects Agency
Contract SD-86
Material Research Program

ARPA SD-86
REPORT E39

May 1967

A Path Independent Integral and the Approximate Analysis of Strain Concentration by Notches and Cracks*

by

James R. Rice**

May 1967

* Support of this research by Brown University and the Advanced Research Projects Agency, under Contract SD-86 with Brown University, is gratefully acknowledged.

** Assistant Professor of Engineering at Brown University.

Abstract

An integral is exhibited which has the same value for all paths surrounding a class of notches in two-dimensional deformation fields of linear or non-linear elastic materials. The integral may be evaluated almost by inspection for a few notch configurations. Also, for materials of the elastic-plastic type (treated through a deformation rather than incremental formulation), with a linear response to small stresses followed by non-linear yielding, the integral may be evaluated in terms of Irwin's stress intensity factor when yielding occurs on a scale small in comparison to notch size. On the other hand, the integral may be expressed in terms of the concentrated deformation field in the vicinity of the notch tip. This implies that some information on strain concentrations is obtainable without recorse to detailed non-linear analyses. Such an approach is exploited here. Applications are made to: 1) Approximate estimates of strain concentrations at smooth ended notch tips in elastic and elastic-plastic materials, 2) A general solution for crack tip separation in the Barenblatt-Dugdale crack model, leading to a proof of the identity of the Griffith theory and Barenblatt cohesive theory for elastic brittle fracture and to the inclusion of strain hardening behavior in the Dugdale model for plane stress yielding, and 3) An approximate perfectly plastic plane strain analysis, based on the slip line theory, of contained plastic deformation at a crack tip and of crack blunting.

Introduction

Consider a homogeneous body of linear or non-linear elastic material free of body forces and subjected to a two dimensional deformation field (plane strain, generalized plane stress, anti-plane strain) so that all stresses σ_{ij} depend only on two cartesian coordinates x_1 (= x) and x_2 (= y) . Suppose the body contains a notch of the type shown in fig. 1, having flat surfaces parallel to the x axis and a rounded tip denoted by the arc Γ_t . A straight crack is a limiting case. Define the strain energy density W by

$$W = W(x,y) = W(\underset{\sim}{\varepsilon}) = \int_0^{\underset{\sim}{\varepsilon}} \sigma_{ij} d\varepsilon_{ij} \quad , \tag{1}$$

where $\underset{\sim}{\varepsilon} = [\varepsilon_{ij}]$ is the infinitesimal strain tensor. Now consider the integral J defined by

$$J = \int_\Gamma \left(W dy - \underset{\sim}{T} \cdot \frac{\partial \underset{\sim}{u}}{\partial x} \, ds \right) \quad . \tag{2}$$

Here Γ is a curve surrounding the notch tip, the integral being evaluated in a contraclockwise sense starting from the lower flat notch surface and continuing along the path Γ to the upper flat surface. $\underset{\sim}{T}$ is the traction vector defined according to the outward normal along Γ , $T_i = \sigma_{ij} n_j$, $\underset{\sim}{u}$ is the displacement vector, and ds is an element of arc length along Γ .

We now prove that the integral J has the same value for all paths Γ .

[redacted]

This path independence, combined with the fact that J can often be directly evaluated, is the key to a variety of subsequent applications to non-linear strain concentration problems. To prove path independence, consider any closed curve Γ^* enclosing an area A^* in a two-dimensional deformation field free of body forces. An application of Green's Theorem [1] in cartesian coordinates $x_1 = x$, $x_2 = y$ gives

$$\int_{\Gamma^*} (W dy - T_i \frac{\partial u_i}{\partial x} ds) = \int_{A^*} [\frac{\partial W}{\partial x} - \frac{\partial}{\partial x_j} (\sigma_{ij} \frac{\partial u_i}{\partial x})] dxdy \quad . \tag{3a}$$

Differentiating the strain energy density,

$$\frac{\partial W}{\partial x} = \frac{\partial W}{\partial \varepsilon_{ij}} \frac{\partial \varepsilon_{ij}}{\partial x} = \sigma_{ij} \frac{\partial \varepsilon_{ij}}{\partial x} \qquad \text{(by eq. 1)}$$

$$= \frac{1}{2} \sigma_{ij} [\frac{\partial}{\partial x} (\frac{\partial u_i}{\partial x_j}) + \frac{\partial}{\partial x} (\frac{\partial u_j}{\partial x_i})] = \sigma_{ij} \frac{\partial}{\partial x_j} (\frac{\partial u_i}{\partial x}) \quad (\text{since } \sigma_{ij} = \sigma_{ji})$$

$$= \frac{\partial}{\partial x_j} (\sigma_{ij} \frac{\partial u_i}{\partial x}) \qquad (\text{since } \frac{\partial \sigma_{ij}}{\partial x_j} = 0) \tag{3b}$$

The area integral in eq. (3a) vanishes identically, and thus

$$\int_{\Gamma^*} (W dy - \underline{T} \cdot \frac{\partial \underline{u}}{\partial x} ds) = 0 \qquad \text{for any closed curve } \Gamma^* \quad . \tag{3c}$$

Path independence of the integral J defined by eq. (2) is now a straightforward consequence. Consider any two paths Γ_1 and Γ_2 surrounding the

notch tip, as does Γ in fig. 1. Traverse Γ_1 in the contraclockwise sense, continue along the upper flat notch surface to where Γ_2 intersects the notch, traverse Γ_2 in the clockwise sense, and then continue along the lower flat notch surface to the starting point where Γ_1 intersects the notch. This describes a closed contour so that the integral of $W dy - \underset{\sim}{T} \cdot (\partial \underset{\sim}{u}/\partial x)\, ds$ vanishes. But $\underset{\sim}{T} = 0$ and $dy = 0$ on the portions of path along the flat notch surfaces. Thus the integral along Γ_1 contraclockwise and the integral along Γ_2 clockwise sum to zero. J has the same value when computed by integrating along either Γ_1 or Γ_2, and path independence is proven. We assume, of course, that the area between curves Γ_1 and Γ_2 is free of singularities.

Our scheme of approach to notch strain concentrations is first to point out in the next section that J can be explicitly evaluated for a variety of configurations and cases. The relation of the integral J to the rate of change of potential energy with respect to notch length will also be noted. Then, in subsequent sections, by appropriate choices of the curve Γ on which J is evaluated, a variety of notch deformation concentration problems will be discussed.

Evaluations of the Integral J

Two special configurations. The integral J may be evaluated almost by inspection for the two special configurations shown in fig. 2. These configurations are not of great practical interest, but are useful in illustrating the relation between the integral J and potential energy variation rates which is taken up below. In fig. 2a, a semi-infinite flat surfaced

notch in an infinite strip of height h, loads are applied by clamping the upper and lower surfaces of the strip so that the displacement vector $\underset{\sim}{u}$ is constant on each clamped boundary. Take Γ to be the dashed curve shown which stretches out to $x = \pm \infty$. There is no contribution to J from the portion of Γ along the clamped boundaries since $dy = 0$ and $\partial \underset{\sim}{u}/\partial x = 0$ there. Also at $x = - \infty$, $W = 0$ and $\partial \underset{\sim}{u}/\partial x = 0$. The entire contribution to J comes from the portion of Γ at $x = + \infty$, and since $\partial \underset{\sim}{u}/\partial x = 0$ there,

$$J = W_\infty h \tag{4}$$

where W_∞ is the constant strain energy density at $x = + \infty$.

Now consider the similar configuration of fig. 2b, with loads applied by couples M per unit thickness on the beam like arms so a state of pure bending (all in-plane stresses vanishing except σ_{xx}) results at $x = - \infty$. For the contour Γ shown by the dashed line, no contribution to J occurs at $x = + \infty$ as W and $\underset{\sim}{T}$ vanish there, and no contribution occurs for portions of Γ along the upper and lower surfaces of the strip as dy and $\underset{\sim}{T}$ vanish. Thus J is given by the integral across the beam arms at $x = - \infty$ and on this portion of Γ, $dy = - ds$, $T_y = 0$, and $T_x = - \sigma_{xx}$. We end up integrating

$$\sigma_{xx} \frac{\partial u_x}{\partial x} - W = \sigma_{xx} \varepsilon_{xx} - W = \sigma_{ij} \varepsilon_{ij} - W$$

$$= \int_0^{\underset{\sim}{\sigma}} \varepsilon_{ij} d\sigma_{ij} = \Omega \tag{5a}$$

across the two beam arms, where Ω is the complimentary energy density. Thus, letting $\Omega_b(M)$ be the complimentary energy per unit length of beam arm per unit thickness for a state of pure bending under moment per unit thickness M,

$$J = 2\Omega_b(M) \quad . \tag{5b}$$

Our motives will be clear enough if we now employ path independence to shrink the curve Γ down to the curved notch tip, denoted by Γ_t in fig. 1. Since the traction vector $\underset{\sim}{T}$ vanishes on the notch surface

$$J = \int_{\Gamma_t} W dy \quad . \tag{6}$$

Without solving generally non-linear and unmanageably difficult boundary value problems, we have extracted a very significant bit of information on the concentrated deformation field at the notch tip. Recognizing W as a function of the surface strain along the tip, we obtain an averaged value of the concentrated strain by simply being able to estimate the strain energy in a homogeneous deformation field, eq. (4), or to solve the problem of pure bending of a beam, eq. (5b). Such simple connections are the essence of the method presented, but we defer the details to subsequent sections and take up next the estimate of J for small zones of notch tip yielding in materials of the elastic-plastic type.

Small scale yielding of elastic-plastic materials. The proof of path independence applies only to elastic materials for which a strain energy density exists. Thus we are here forced to consider deformation theories of plasticity (non-linear elasticity) rather than the physically more appropriate incremental theories. This should not be a great drawback [2,3] for problems of monotonic loading. Specifically, we shall here understand the phrase "elastic-plastic material" to mean an elastic material exhibiting a linear Hookian response to stresses inside some initial yield surface in stress space, and a non-linear (strain hardening) response to stresses outside the initial yield surface. We consider a narrow crack-like notch and derive a formula for the integral J when the yielded zone is confined to a small region near the notch tip that is negligible in size in comparison to geometric dimensions such as notch length, unnotched specimen width, etc.

The situation envisioned has been termed "small scale yielding" [2,4,5], and we employ a special boundary layer type formulation of the problem developed in work by the author [2,5] and others [6,7], and described most fully in a recent survey [8] on crack plasticity. The essential ideas are illustrated in reference to fig. 3. Loadings symmetrical about the narrow notch are imagined to induce a deformation state of plane strain. First, consider the linear elastic solution of the problem when the notch is presumed to be a sharp crack. Employing polar coordinates r,θ with origin at the crack tip, the form of stresses in the vicinity of the tip are known [9-11] to exhibit a characteristic inverse square root dependence on r :

$$\sigma_{ij} = \frac{K_I}{(2\pi r)^{1/2}} f_{ij}(\theta) + \text{other terms which are bounded at the crack tip.} \qquad (7a)$$

Here the set of functions $f_{ij}(\theta)$ are the same for all symmetrically loaded crack problems, and for the isotropic material [9,10,12]

$$f_{xx}(\theta) = \cos(\theta/2)\,[1 - \sin(\theta/2)\sin(3\theta/2)]$$

$$f_{yy}(\theta) = \cos(\theta/2)\,[1 + \sin(\theta/2)\sin(3\theta/2)] \qquad (7b)$$

$$f_{xy}(\theta) = f_{yx}(\theta) = \sin(\theta/2)\cos(\theta/2)\cos(3\theta/2) \quad .$$

K_I is Irwin's stress intensity factor [10,12], a function of geometry and applied load, depending linearly on the latter, that has been tabulated [12] for a wide variety of crack configurations on the basis of extensive recent elastic crack solutions generated in studies on fracture mechanics. Now suppose the material is elastic-plastic, the flat surfaced notch is either a sharp crack or a narrow void, and the load level is sufficiently small so that a yield zone forms near the tip which is small compared to notch length and similar characteristic dimensions (small scale yielding, fig. 3a). One anticipates that the elastic singularity governs stresses at distances from the notch root that are large compared to yield zone and root radius dimensions but still small compared to characteristic geometric dimensions such as notch length. The actual configuration of fig. 3a is then replaced by the simpler semi-infinite notch in an infinite body (fig. 3b), and a boundary layer approach is employed replacing actual boundary conditions in fig. 3a with the asymptotic boundary conditions

$$\sigma_{ij} \to \frac{K_I}{(2\pi r)^{1/2}}\, f_{ij}(\theta) \qquad \text{as} \quad r \to \infty \quad , \qquad (7c)$$

where K_I is the stress intensity factor from the linear elastic crack solution.

Such boundary layer solutions for cracks are mathematically exact in the plastic region only to the first nonvanishing term of a Taylor expansion of complete solutions in the applied load [2,4,5]. But comparison [8] with available complete solutions indicates the boundary layer approach to be a highly accurate approximation up to substantial fractions (typically, one-half) of net section yielding load levels. We now evaluate the integral J (eq. 2) from the boundary layer solution, taking Γ to be a large circle of radius r in fig. 3b :

$$J = r \int_{-\pi}^{+\pi} [W(r,\theta) \cos \theta - \underset{\sim}{T}(r,\theta) \cdot \frac{\partial \underset{\sim}{u}}{\partial x}(r,\theta)] \, d\theta \quad . \tag{8a}$$

By path independence we may let $r \to \infty$ and since W is quadratic in strain in the elastic region, only the asymptotically approached inverse square root elastic stress field (eq. 7c) contributes. Working out the associated plane strain deformation field, one finds

$$J = \frac{1 - \nu^2}{E} K_I^2 \quad \text{for small scale yielding} \, , \tag{8b}$$

where E is Young's modulus and ν Poisson's ratio. We have thus evaluated J for an infinite variety of problems, and made an unexpected use of linear elastic crack solutions in elastic-plastic problems.

Primarily, we will later deal with one configuration, the notch of length $2a$ in a remotely uniform stress field σ_∞ (fig. 4). Here [10]

$$K_I = \sigma_\infty (\pi a)^{1/2} \quad \text{and} \quad J = \frac{\pi(1 - \nu^2)}{E} \sigma_\infty^2 a \quad \text{for small scale yielding} \tag{9}$$

For plane stress, the same result holds for J with $1 - \nu^2$ replaced by unity. Thus far only loadings symmetrical about the narrow notch line have been considered (the opening mode in Irwin's terminology [10]). The same computation may be carried out for more general loadings. Letting K_I, K_{II}, and K_{III} be elastic stress intensity factors [10] for the opening, in-plane sliding, and anti-plane sliding modes, respectively, of notch tip deformation one readily obtains

$$J = \frac{1 - \nu^2}{E} (K_I^2 + K_{II}^2) + \frac{1 + \nu}{E} K_{III}^2 \quad \text{(small scale yielding)} \tag{10}$$

A physical interpretation in terms of energy comparisons for notches of neighboring size. In view of the path independence it should come as little surprise that a simple physical interpretation can be attached to J. Consider the two dimensional deformation of a body with cross section A' and bounding curve Γ'. Letting Γ'' be that portion of Γ' on which non-vanishing tractions $\underset{\sim}{T}$ are prescribed, we define the potential energy per unit thickness by

$$P = \int_{A'} W \, dxdy - \int_{\Gamma''} \underset{\sim}{T} \cdot \underset{\sim}{u} \, ds \, . \tag{11}$$

Suppose the body contains a flat surfaced notch, as in fig. 1, with a tip at $x = \ell$ and denote the potential energy by $P(\ell)$. We compare this with the potential energy $P(\ell + \Delta\ell)$ of a body identical in every respect (same shape and same distribution of prescribed displacements and/or tractions on the boundary), except that the notch is longer with the tip now at a neighboring position $x = \ell + \Delta\ell$. The shape of the curved notch tip Γ_t is imagined the same in both cases. Then one may show that the integral J defined by eq. (2) is

$$J = -\lim_{\Delta\ell \to 0} \frac{P(\ell + \Delta\ell) - P(\ell)}{\Delta\ell} = -\frac{\partial P}{\partial \ell} , \tag{12}$$

the rate of decrease of potential energy with respect to notch length under fixed prescribed boundary values. The proof is fairly long, and is deferred to a subsequent report both in the interests of brevity and because a direct focus on energy variations is a subject in itself allowing a variety of further results on non-linear strain concentrations at notches. For the present, we simply note below that J does indeed equal the potential energy decrease rate for the cases evaluated above.

When loading is entirely by prescribing boundary displacements as in fig. 2a, the potential energy equals the strain energy and we check from eq. (4) that J is indeed equal to the rate of decrease of strain energy with respect to notch length. When loading is entirely by prescribing boundary tractions as in fig. 2b, a simple application of virtual work in eq. (11) shows that the potential energy equals minus the complimentary energy, and eq. (5b) checks J to be the rate of increase of complimentary energy with respect to notch length. Readers familiar with elastic fracture mechanics

will recognize eqs. (8b-10) as giving results for J which are identical to the potential energy decrease rate calculated in general form by Irwin [10] in terms of his stress intensity factors for linear elastic crack problems. When deviations from linearity occur over a region negligible in comparison to characteristic dimensions of a problem (small scale yielding), it is clear that the energy decrease rate should be insensitive to the yielding and thus still given by the linear elastic expressions so that we again check eq. (12). The physical interpretation of J in terms of a variation rate in potential energy is useful in enabling an approximate treatment of notch strain concentrations when yielding is not confined to a small region near the tip. For example, suppose we can solve a simplified elastic-plastic model for yielding near a notch. Even though the solution may be very wrong in detail, we might confidently expect the model to accurately predict a gross feature of the solution such as the rate of variation of potential energy with respect to notch length. Thus we compute J from the simplified model, and then ignore the model and go on to employ techniques of the next sections to analyze strain concentrations at the notch tip. Examples are discussed subsequently.

Strain Concentrations at Smooth Ended Notches

When we shrink the contour Γ down to the curved tip Γ_t of a smooth ended notch, as in deriving eq. (6), there results

$$J = \int_{\Gamma_t} W dy = \int_{-\pi/2}^{+\pi/2} W(\phi)\, r_t(\phi) \cos\phi \, d\phi \quad . \tag{13}$$

Here ϕ is the angle between the tangent line at a point on the curved tip and the y axis (fig. 5) and $r_t(\phi)$ is the radius of curvature at that point. Viewing J as a known function of the applied load, we obtain an approximate estimate of the maximum concentrated strain by choosing some reasonable dependence of the strain energy on ϕ. Some guidance on what constitutes a reasonable choice is given by a perusal of known solutions for notches.

A well known [13] feature of the linear elastic problem of an ellipsoidal inclusion imbedded in a matrix of another material, subjected to a uniform remote stress state, is that the inclusion undergoes a homogeneous deformation. Strains in the inclusion are independent of position. The ellipsoidal void is a limiting case with an inclusion of zero elastic modulus, surface strains being compatible with a homogeneous deformation of the imagined zero-modulus inclusion. Now consider the special case of a narrow elliptical void symmetrically loaded under plane strain conditions. Let ε_{max} be the maximum extensional strain, occurring at the notch tip on the semi-major axis. Then the imagined inclusion undergoes a homogeneous strain $\varepsilon_{yy} = \varepsilon_{max}$ and $\varepsilon_{xx} = \varepsilon_{min}$, where ε_{min} is the surface extensional strain on the semi-minor axis. The latter is negligible in comparison to ε_{max} for a narrow ellipse and essentially the inclusion undergoes a single homogeneous strain ε_{max} in the y direction. Matching surface extensional strain ε with extensional strain in the imagined zero modulus inclusion in a direction tangent to the void boundary,

$$\varepsilon = \varepsilon_{max} \cos^2 \phi \qquad \text{when } \varepsilon_{min} \text{ is negligible} , \tag{14a}$$

where ϕ is the tangent angle introduced in fig. 5.

As an approximation for our flat surfaced notch problems, we may consider the deformation of the notch surface near the tip to be describable by the homogeneous straining of an imagined zero modulus inclusion. Thus the maximum concentrated strain is estimated from eqs. (13,14a) by setting

$$J \approx \int_{-\pi/2}^{+\pi/2} W(\varepsilon_{max} \cos^2 \phi)\, r_t(\phi) \cos \phi \, d\phi \quad . \tag{14b}$$

Here $W(\varepsilon)$ is the strain energy accompanying an extensional strain ε on the notch surface. One might instead presume that the distribution of strain energy with ϕ in the linear elastic ellipse problem,

$$W = W(\varepsilon_{max}) \cos^4 \phi \qquad \text{when } \varepsilon_{min} \text{ is negligible} \quad , \tag{15a}$$

is more likely to be a better approximation for our flat surfaced notch problems. In this case the maximum strain is estimated from

$$J \approx W(\varepsilon_{max}) \int_{-\pi/2}^{+\pi/2} \cos^5 \phi \, r_t(\phi) \, d\phi \quad . \tag{15b}$$

Certainly, neither assumption is exact and there is no way (without recourse to the detailed solutions we are trying to avoid) to decide which gives the best answer. As we shall see, resulting answers for maximum strain are somewhat sensitive to our choice. An examination of some results from known anti-plane strain solutions does, however, suggest that eq. (14b) be

employed. If we consider the elliptical void subjected to symmetrical anti-plane strain loadings, the imagined zero modulus inclusion undergoes the homogeneous strain $\varepsilon_{yz} = \gamma_{max}/2$ where γ_{max} is the maximum concentrated "engineering" shear strain occurring at the notch tip. Matching shear strains γ on the notch surface with shears in the inclusion

$$\gamma = \gamma_{max} \cos \phi \quad . \tag{16a}$$

It happens that a solution for a crack in a uniform remotely applied anti-plane stress field has been given [2,6] for elastic-plastic materials with arbitrary non-decreasing relations between stress and strain in the plastic range. Neuber [6] first pointed out that such crack solutions also give solutions for a family of smooth ended notches since stress trajectories in the crack solution may be thought of as traction free notch surfaces. Methods of locating such notch boundaries are discussed in [8]. If we take the small scale yielding solution [2] in which the crack is viewed as semi-infinite and generate the family of smooth ended semi-infinite notches by methods of [8], the surprising result turns out that eq. (16a) is satisfied on the notch surface regardless of the relation between stress and strain in the plastic range. Recalling that small scale yielding solutions give details correctly only near the notch tip, the assumption of a homogeneously deformed zero modulus inclusion accurately describes deformations of the notch tip at least at low load levels. The shape of notch surfaces generated by stress trajectories of the crack solution do depend on the stress-strain relation. Parabolas result for linear elastic behavior. Perfectly plastic behavior leads to a semi-circular notch

tip [8] where the stress trajectories pass through the crack plastic zone, and relatively flat notch surfaces where the trajectories pass through elastic material. This is especially encouraging as our formulation is for flat surfaced notches and our main interest is with ductile materials.

Neuber [6] pointed out for this class of anti-plane strain problems that the product of stress and strain concentration factors is independent of the stress-strain relation. A more careful examination of mathematical results [8] indicated the Neuber result to be valid only for small scale yielding of elastic-plastic materials, and only for the comparison of stress and strain concentrations at notch tips whose geometry does depend on the stress-strain relations. Thus the Neuber result is only approximately correct. Rather, our present considerations of path independent integrals and their relation to potential energy variations appear to be the embracing principles which lead to Neuber's result in special cases. If we approximate notch tip deformations by eq. (16a) in anti-plane strain problems, the maximum concentrated strain is estimated from

$$J \approx \int_{-\pi/2}^{+\pi/2} W(\gamma_{max} \cos \phi)\, r_t(\phi) \cos \phi \, d\phi \quad , \tag{16b}$$

where $W(\gamma)$ is the strain energy accompanying an anti-plane strain γ of the notch surface. Strict equality holds for notch surfaces generated by stress trajectories of the small scale yielding crack solution, with J set equal to its linear elastic value (last term of eq. 10).

Having received some encouragement from the anti-plane strain case, we now proceed to use eq. (14b) (homogeneous deformation of void interior in the neighborhood of the notch tip) to estimate concentrated deformations in the plane straining of a flat surfaced notch with a semi-circular tip ($r_t(\phi) = r_t$ = a constant). We shall always first give results in terms of J and then, to put equations in more familiar terms, give results for the special value of J in eq. (9) for small scale yielding near the narrow notch of length $2a$ in a uniform remote stress field σ_∞ (fig. 4). The reader should recall, however, that J is known either approximately or exactly for a large number of other cases and configurations.

For linear elastic behavior stress-strain relations and strain energy density on the notch surface under plane strain conditions are

$$\sigma = \frac{E}{1 - \nu^2}\,\varepsilon \quad , \qquad W(\varepsilon) = \frac{E\varepsilon^2}{2(1 - \nu^2)} \quad . \tag{17a}$$

Inserting in eq. (14b) and solving for the maximum concentrated strain,

$$\varepsilon_{max} \approx \left[\frac{15(1 - \nu^2)\,J}{8E\,r_t}\right]^{1/2} = 2.43\,\frac{(1 - \nu^2)\,\sigma_\infty}{E}\left(\frac{a}{r_t}\right)^{1/2} \quad . \tag{17b}$$

The numerical factor of 2.43 appears appropriate for a flat surfaced notch when one recalls the factor 2.00 for the narrow elliptical hole [14] of the same root radius. The ellipse represents a much less abrupt transmission of load around the notch tip (the ratio of semi-minor axis length to root radius

approaches infinity as the ellipse is narrowed toward zero thickness). For perfectly plastic behavior, let σ_Y be the yield stress at points along the notch surface under plane strain conditions. With elastic compressibility a limiting yield stress in plane strain is really approached asymptotically when plastic strains become large compared to elastic strains [15], but we shall consider a simple picture of linear behavior up to σ_Y and constant stress thereafter. Then

$$\sigma = \sigma_Y \quad , \quad W(\varepsilon) = \sigma_Y (\varepsilon - \varepsilon_Y) + \frac{1}{2} \sigma_Y \varepsilon_Y \quad , \quad \text{for} \quad \varepsilon > \varepsilon_Y \quad , \tag{18a}$$

and eq. (17a) applies for $\varepsilon < \varepsilon_Y$, where

$$\varepsilon_Y = \frac{(1 - \nu^2)\, \sigma_Y}{E} \tag{18b}$$

is the yield strain given by Hooke's law under plane strain conditions. One then obtains from eq. (14b), when the yield strain is exceeded,

$$\left(\frac{\varepsilon_{max}}{\varepsilon_Y}\right)^2 - \left(\frac{\varepsilon_Y}{\varepsilon_{max}}\right)^{1/2} \left(\frac{\varepsilon_{max}}{\varepsilon_Y} - 1\right)^{5/2} \approx \frac{15\, J}{8 \sigma_Y \varepsilon_Y r_t} = \frac{15\, \pi}{8} \left(\frac{\sigma_\infty}{\sigma_Y}\right)^2 \frac{a}{r_t} \, . \tag{18c}$$

This equation, along with the linear elastic result, is plotted as the solid curve in fig. 6. The ratio of maximum concentrated strain to yield strain is shown as a function of the square root of the terms on the right in eq. (18c),

since this dimensionless representation of the applied load has the value unity at initial yield and, at least at low load levels when J is given by the linear elastic expression of eqs. (8,9), is linear in the applied load. The left side of the above equation may be developed in a series, and if we neglect all terms which vanish when $\varepsilon_{max}/\varepsilon_Y >> 1$,

$$\varepsilon_{max} \approx \frac{3}{4}\left(\varepsilon_Y + \frac{J}{\sigma_Y r_t}\right) = .075\ \varepsilon_Y + 2.36\ \varepsilon_Y \left(\frac{\sigma_\infty}{\sigma_Y}\right)^2 \frac{a}{r_t} \ . \qquad (18d)$$

This equation gives a result for the maximum concentrated strain which is 15% too large at the initial yield load; the discrepancy with eq. (18c) becomes imperceptible at loads greater than three times the initial yield load.

Strain hardening poses no special difficulty with our present method. For simplicity of resulting formulae, we shall limit attention to cases where concentrated strains are very large compared to the initial yield strain. Thus, for linear work hardening in the relation between stress and strain on the notch surface,

$$\sigma = \sigma_Y + \frac{E_w}{1-\nu^2}(\varepsilon - \varepsilon_Y) \quad , \quad \varepsilon > \varepsilon_Y \ , \qquad (19a)$$

eq. (14b) leads to

$$\varepsilon_{max} \approx \frac{5}{4}\frac{E}{E_w}\varepsilon_Y \left\{\left[1 + \frac{6\ E_w\ J}{5\ \varepsilon_Y E \sigma_Y r_t}\right]^{1/2} - 1\right\}$$

$$\approx \frac{5}{4}\frac{E}{E_w}\varepsilon_Y \left\{\left[1 + \frac{6\pi}{5}\frac{E_w}{E}\left(\frac{\sigma_\infty}{\sigma_Y}\right)^2 \frac{a}{r_t}\right]^{1/2} - 1\right\} \qquad (19b)$$

Here E_w is the tangent modulus (effectively) and terms of order $\sigma_Y\varepsilon_Y$ and $E_w\varepsilon_Y\varepsilon$ have been neglected in the expression for the energy density, as appropriate for large strains and for $E_w << E$. For a power law relating stress and strain on the notch surface in the hardening range,

$$\sigma = \sigma_Y (\varepsilon/\varepsilon_Y)^N \quad , \quad \varepsilon > \varepsilon_Y \quad , \tag{20a}$$

eq. (14b) results in

$$\varepsilon_{max} \approx \varepsilon_Y \left[\frac{(N+1/2)\ (N+3/2)\ \Gamma\ (N+1/2)}{\Gamma\ (1/2)\ \Gamma\ (N+1)} \quad \frac{J}{\varepsilon_Y \sigma_Y r_t} \right]^{1/(1+N)}$$

$$\approx \varepsilon_Y \left[\frac{\pi\ (N+1/2)\ (N+3/2)\ \Gamma\ (N+1/2)}{\Gamma\ (1/2)\ \Gamma\ (N+1)} \quad \left(\frac{\sigma_\infty}{\sigma_Y}\right)^2 \quad \frac{a}{r_t} \right]^{1/(1+N)} , \tag{20b}$$

where $\Gamma(..)$ is the Gamma Function. Again terms of order $\sigma_Y\varepsilon_Y$ have been neglected in the energy density.

The reader is cautioned again that the latter forms in expressions above for ε_{max} apply only to the vase of small scale yielding near the narrow notch of length $2a$ in fig. 4 (that is, for σ_∞ less than approximately half of σ_Y); we consider approximations for large scale yielding later. Also, we have approximated strains on the notch surface by requiring compatibility with the homogeneous deformation of the void interior, eq. (14b). Had we assumed instead that the energy density distribution remains the same as for the linear

elastic elliptical void problem, eq. (15b), larger values for ε_{max} would be obtained in all cases except the linear elastic. The largest difference occurs in the elastic-perfectly plastic case, for which eq. (15b) leads to

$$\varepsilon_{max} \approx \frac{1}{2}\left(\varepsilon_Y + \frac{15\ J}{8\sigma_Y r_t}\right) = 0.50\ \varepsilon_Y + 2.95\ \varepsilon_Y \left(\frac{\sigma_\infty}{\sigma_Y}\right)^2 \frac{a}{r_t} \qquad (21)$$

for loads greater than the initial yield value. The equation is shown by the upper dashed curve in fig. 6. The difference with eq. (18c), based on homogeneous deformation of the void interior, approaches 25% when the concentrated strain is large compared to the yield strain.

A lower bound on the maximum concentrated strain is readily established, for

$$J = \int_{\Gamma_t} W dy \leq W(\varepsilon_{max}) \int_{\Gamma_t} dy = 2r_t\, W(\varepsilon_{max}) , \qquad (22a)$$

with the latter form for a semi-circular tip.

For the elastic-perfectly plastic case, the resulting inequality is

$$\varepsilon_{max} \geq \frac{1}{2}\left(\varepsilon_Y + \frac{J}{\sigma_Y r_t}\right) = 0.50\ \varepsilon_Y + 1.57\ \varepsilon_Y \left(\frac{\sigma_\infty}{\sigma_Y}\right)^2 \frac{a}{r_t} \qquad (22b)$$

whenever the load is large enough for the right side of the inequality to exceed ε_Y. This lower bound, along with the lower bound resulting in the elastic range, is shown by the lower dashed curve in fig. 6.

The Barenblatt-Dugdale Crack Model

Sharp cracks lead to strain singularities. The Griffith theory of brittle fracture [16,17,10] ignores the unrealistic prediction of conditions at the crack tip, and employs an energy balance to set the potential energy decrease due to crack extension equal to the surface energy of the newly created crack faces. An alternate approach due to Barenblatt [18] removes the singularity by considering a cohesive zone ahead of the crack, postulating that the influence of molecular or atomic attractions is representable as a restraining stress acting on the separating surfaces, fig. 7. The restraining stress $\sigma = \sigma(\delta)$ is a function of separation distance δ as in fig. 7b. Dugdale [19] employed the same model to discuss plane stress yielding near cracks in thin sheets. As further studies have verified [20], yielding is limited to a narrow slit-like zone ahead of the crack of height approximately equal to sheet thickness when the plastic cohesive zone is large compared to thickness. Except for a perturbation near the tip, yielding then consists of slip on 45° planes through the thickness so that the plastic strain is essentially the separation distance divided by the sheet thickness. Restraining stresses typical of plane stress yielding are shown in fig. 7c.

We may evaluate our integral J of eq. (2) by employing path independence to shrink the contour Γ down to the lower and upper surfaces of the cohesive zone as in fig. 7a. Then since $dy = 0$ on Γ ,

$$J = -\int_{\Gamma} \underset{\sim}{T} \cdot \frac{\partial \underset{\sim}{u}}{\partial x}\, ds$$

$$= -\int_{\text{cohes. zone}} \sigma(\delta)\, \frac{d\delta}{dx}\, dx = -\int_{\text{cohes. zone}} \frac{d}{dx} \left\{ \int_0^{\delta} \sigma(\delta)\, d\delta \right\} dx$$

$$= \int_0^{\delta_t} \sigma(\delta)\, d\delta \qquad (23)$$

where δ_t is the separation distance at the crack tip. Thus, if the crack configuration is one of many for which J is known, we are able to solve for the crack opening displacement directly from the force-displacement curve.

Now let us compare the Griffith theory of elastic brittle fracture with the fracture prediction from the Barenblatt type cohesive force model. Letting δ^* be the separation distance in fig. 7b when the atoms at the crack tip can be considered pulled out of range of their neighbors, the value of J which will just cause crack extension (or, if crack extension is considered as reversible, will maintain equilibrium at the current crack length) is then

$$J = \int_0^{\delta^*} \sigma(\delta)\, d\delta \qquad \text{(cohesive theory)} \qquad (24a)$$

On the other hand, the Griffith theory regards the total potential energy of a cracked body as $P + 2\,S\,\ell$, where ℓ is crack length, S is surface energy, and P is the potential energy defined by the continuum mechanics solution without regard to cohesive forces. Determining equilibrium by setting the variation in total potential to zero,

$$-\frac{\partial P}{\partial \ell} = 2S \qquad \text{(Griffith Theory)} \qquad (24b)$$

We conclude that the Griffith theory is identical to a theory of fracture based on atomic cohesive forces, regardless of the force-attraction law, so long as the usual condition is fulfilled that the cohesive zone be negligible in size compared to characteristic dimensions (small scale yielding). This is because the area under the force-separation curve is by definition twice the surface energy and, as we have noted, J is equal to the potential energy decrease rate for small scale yielding.

Strain hardening behavior is also readily included in the Dugdale model; analyses to date have been limited to perfect plasticity. For example, with linear work hardening

$$\sigma(\delta) = \sigma_Y + E_w \frac{\delta}{h} \qquad (25a)$$

where h is sheet thickness, E_w a tangent modulus, and the strain approximated by δ/h, eq. (23) gives the crack opening displacement as

$$\delta_t = \frac{\sigma_Y h}{E_w} \left\{\left(1 + \frac{2 E_w J}{h \sigma_Y^2}\right)^{1/2} - 1\right\}$$

$$= \frac{\sigma_Y h}{E_w} \left\{\left[1 + 2\pi \frac{E_w}{E} \left(\frac{\sigma_\infty}{\sigma_Y}\right)^2 \frac{a}{h}\right]^{1/2} - 1\right\} . \qquad (25b)$$

In the latter form the plane stress value of J for the crack of length $2a$, appropriate for small scale yielding, has been used. With negligible strain

hardening ($E_w = 0$) this becomes

$$\delta_t = \frac{J}{\sigma_Y} = \frac{\pi \sigma_\infty^2 a}{E \sigma_Y} \tag{25c}$$

as is obvious from eq. (23). The simple picture of plane stress yielding in the Dugdale model is correct only at distances from the crack tip greater than the sheet thickness, approximately, with a truly three dimensional deformation state prevailing very near the crack tip [20]. However, in thin sheets with the plastic zone extending over a distance several times the thickness, estimates of crack opening displacements may be expected to be reasonably accurate as the tip displacement is an integrated effect of plastic straining along the entire length of the plastic zone. Experimental confirmations of perfectly plastic predictions for plastic zone sizes [19] and crack opening displacements [20] have been satisfactory, and opening displacements have proven a useful, if imperfect, measure of the severity of local deformations in the formulation of fracture criteria [21].

Complete solutions of the Barenblatt-Dugdale model have been given for the case of a constant cohesive stress σ_0 acting whenever the separation distance δ is non-zero. The resulting opening displacement for the crack of length $2a$ in a uniform stress field, fig. 4, is [4]

$$\delta_t = \frac{8 (1 - \nu^2) \sigma_0}{\pi E} \log \left[\sec \left(\frac{\pi \sigma_\infty}{2 \sigma_0} \right) \right] \tag{26a}$$

for plane strain, with the $1 - \nu^2$ factor removed for plane stress. But

since $\delta_t = J/\sigma_0$ from eq. (23), we can solve for J to find

$$J = \frac{8\,(1 - \nu^2)\,\sigma_0^{\,2}}{\pi E} \log \left[\sec \left(\frac{\pi\,\sigma_\infty}{2\,\sigma_0} \right) \right] .$$

Expanding the logarithm secant term in a series and retaining only the first non-vanishing term, as appropriate when σ_∞/σ_0 is small, we obtain the linear elastic expression for J of eq. (9) and verify our procedure of using the linear elastic expressions in cases of small scale yielding. Solutions of the Barenblatt-Dugdale model with constant cohesive stress have been given for other configurations of single cracks in infinite bodies [4], including wedge force loadings, and for an infinite periodic array of collinear cracks [22], an approximation for single edge, double edge, and central cracks in finite width plates. Crack opening displacements from these solutions may be used to compute J, as in eqs. (26). In view of the physical interpretation given J as an energy variation rate, we do not expect resulting expressions to be too tied to the model. Thus, after a judicious choice of σ_0 to account for possible hydrostatic stress elevations of plastic limit loads as in the double edge notched plate [23], Barenblatt-Dugdale estimates of J may be used as an approximation in cases of large scale yielding for computations such as those of the last section. Fig. 8 shows a comparison of the linear elastic (eq. 9) and constant cchesive stress Barenblatt-Dugdale (eq. 26b) expressions for J for the configuration of fig. 4. The plot is in dimensionless form, with $E\,J/[\pi(1 - \nu^2)\,\sigma_0^{\,2}]$ shown as a function of the applied stress ratio σ_∞/σ_0. The linear elastic (small scale yielding) result is a parabola

with the dimensionless J equal to the square of the stress ratio. The closeness of the two curves at low stress levels indicates the great usefulness of the small scale yielding approximation.

Because it will be useful for a later comparison with plane strain plasticity, we record here the expression for the length of the cohesive zone in the case of constant cohesive stress σ_0 and the crack of length $2a$ in a uniform stress field. Letting R be the cohesive zone length, the result is [4]

$$R = a\left[\sec\left(\frac{\pi\sigma_\infty}{2\sigma_0}\right) - 1\right] \approx \frac{\pi^2}{8} a \left(\frac{\sigma_\infty}{\sigma_0}\right)^2 . \qquad (26c)$$

The latter form is the first term in a Taylor expansion. Again we verify that the elastic stress intensity factor (eq. 9) controls inelastic behavior in the small scale yielding range. Setting $\sigma_0 = \sigma_Y$ (the yield stress in tension), R is the plastic zone size in plane stress predicted by the Dugdale model. The model is valid when the computed value of R is several times the sheet thickness.

Other known elastic-plastic solutions for cracks and notches may be used to estimate J for cases of large scale yielding. In particular the many available perfectly plastic [5,7,8] and strain hardening [2,6,8] solutions for cracks in anti-plane stress fields may be put to use. Resulting detailed evaluations of J are deferred in the interest of brevity. It is simply noted here that in all cases the validity of our small scale yielding result (last term of eq. 10) is confirmed, and that in the perfectly plastic case the large

scale yielding range prediction of the deviation of J from the small scale yielding formula is not significantly different from that of the Barenblatt-Dugdale model.

Plane Strain Yielding Near a Crack

An approximate treatment of perfectly plastic plane strain yielding near a crack may be based on the slip line theory [15] and our considerations of path independence. Slip line theory is really a valid consequence of a Tresca or Mises yield criterion only when elastic straining is incompressible or when plastic strains greatly exceed initial yield strains. However, we shall see that it is appropriate for our present purposes. Suppose tentatively that the plastic region completely surrounds the crack tip as in fig. 9. The exact shape of the elastic-plastic boundary is unknown, as indicated by the question mark. The traction free boundary condition on the crack surface determines a constant stress state in the largest isosceles right triangle (A in fig. 9) which may be fit into the plastic zone, and in this region

$$\sigma_{xx} = 2\,\tau_Y \quad , \quad \sigma_{yy} = \sigma_{xy} = 0 \qquad \text{(region A)} \tag{27a}$$

where τ_Y is the yield stress in pure shear. We choose tension instead of compression for σ_{xx} since the latter choice would result in biaxial compression ahead of the crack. Any slip line emanating from the crack surface and finding its way to the x axis in front of the crack must swing through an angle of $\pi/2$. Thus a hydrostatic stress elevation of $2\,\tau_Y(\pi/2)$ must

result ahead of the crack [15]. Constant stresses on this line determines a constant stress state in a diamond shaped region (B in fig. 9), and there

$$\sigma_{xx} = \pi\tau_Y \quad , \quad \sigma_{yy} = (2 + \pi)\,\tau_Y \quad , \quad \sigma_{xy} = 0 \quad \text{(region B)} . \tag{27b}$$

A centered fan (C in fig. 9) must join two such regions of constant stress [15,24] and stresses in the fan are

$$\sigma_{rr} = \sigma_{\theta\theta} = (1 + \frac{3\pi}{2})\,\tau_Y - 2\tau_Y\theta \quad , \quad \sigma_{r\theta} = \tau_Y \quad \text{(region C)}. \tag{27c}$$

The resulting slip line field is familiar in the limit analysis of rigid indentors [15,24] and double edge notched thick plates [23,25].

Large strains can occur only when slip lines focus, as in the centered fan, but not in constant state regions (A and B) unless strains are uniformly large along the straight slip lines and thus out toward the elastic-plastic boundary (where strains must be small). One then anticipates strains on the order of initial yield values in the constant state regions. As we shall see, only the strain singularity in the centered fan enters the results we are heading toward. Assuming elastic incompressibility and agreement between principal shear stress and strain directions, $\varepsilon_{rr} = \varepsilon_{\theta\theta} = 0$ in the centered fan. This implies that displacement components are there representable in the form [15,24]

$$u_r = f'(\theta) \quad , \quad u_\theta = -f(\theta) + g(r) \tag{28a}$$

Note that in a proper incremental theory, these equations apply to velocities instead of displacements. The shear strain $\varepsilon_{r\theta}$ in the centered fan is given by

$$\varepsilon_{r\theta} = \frac{1}{2}\left(\frac{1}{r}\frac{\partial u_r}{\partial \theta} + \frac{\partial u_\theta}{\partial r} - \frac{u_\theta}{r}\right) = \frac{f''(\theta) + f(\theta) - g(r)}{2r} + \frac{1}{2}g'(r) \quad . \tag{28b}$$

Now consider the path independent integral J, eq. (2). Taking Γ to be a circle of radius r centered at the crack tip and expressing all quantities in polar component form, there results

$$J = r\int_{-\pi}^{+\pi} \{W\cos\theta - \sigma_{rr}[\varepsilon_{rr}\cos\theta - (\varepsilon_{r\theta} - \omega)\sin\theta] - \sigma_{r\theta}[(\varepsilon_{r\theta} + \omega)\cos\theta - \varepsilon_{\theta\theta}\sin\theta]\}\, d\theta \quad . \tag{29a}$$

Here ω is the rotation, measured positive contraclockwise:

$$\omega = \frac{1}{2}\left(\frac{\partial u_\theta}{\partial r} + \frac{u_\theta}{r} - \frac{1}{r}\frac{\partial u_r}{\partial \theta}\right) \quad . \tag{29b}$$

We evaluate the integral by letting $r \to 0$ (as permitted by path independence). Since strains are non-singular in the constant state regions, only the portion of the integral taken over the centered fans ($\pi/4 < |\theta| < 3\pi/4$) contributes in the limit. We now express the energy density, strains, and rotation in a form appropriate when $r \to 0$. First note that arbitrarily we

may set $f(\pi/4) = 0$. Then $g(r)$ represents the θ direction displacement of the straight line boundary between regions B and C in fig. 9 . Since strains are bounded in the constant state region, the displacement is zero at $r = 0$ and $\theta = \pm\pi/4$. Thus

$$g(0) = 0 \qquad \text{and} \qquad g'(0) = \lim_{r \to 0} \frac{g(r)}{r} \quad , \tag{30a}$$

and expressions for displacements, strains, and rotation very near the crack tip become

$$u_r = f'(\theta) \quad , \quad u_\theta = -f(\theta) \qquad (f(\pi/4) = f'(\pi/4) = 0)$$

$$\varepsilon_{rr} = \varepsilon_{\theta\theta} = 0 \quad , \quad \varepsilon_{r\theta} = -\omega = \frac{f''(\theta) + f(\theta)}{2r} \tag{30b}$$

The energy density for an elastically incompressible perfectly plastic material is

$$W = \frac{1}{2} G\gamma^2 \quad (\gamma < \gamma_Y) \quad , \quad W = \tau_Y \gamma - \frac{1}{2} \tau_Y \gamma_Y \quad (\gamma > \gamma_Y) \quad . \tag{31a}$$

Here $\gamma_Y = \tau_Y/G$ is the "engineering" yield strain in shear and

$$\gamma = \left[(\varepsilon_{rr} - \varepsilon_{\theta\theta})^2 + 4\varepsilon_{r\theta}^2 \right]^{1/2} \tag{31b}$$

is the principal shear strain. We may see that the expression given for W

when $\gamma > \gamma_Y$ is correct in the sense that any set of stresses satisfying $dW = \sigma_{ij} d\varepsilon_{ij}$ also satisfies the Mises or Tresca yield condition and gives a common ratio of deviatoric stress components to deviatoric strain components. Thus as $r \to 0$ in the centered fans

$$W = \tau_Y \frac{f''(\theta) + f(\theta)}{r} \quad . \tag{31c}$$

Letting $r \to 0$ in eq. (29a), the result for J then becomes

$$J = 2\tau_Y \int_{\pi/4}^{3\pi/4} [f''(\theta) + f(\theta)] \left[\cos\theta + \left(1 + \frac{3\pi}{2} - 2\theta\right) \sin\theta\right] d\theta \tag{32}$$

Regarding J as known, we get an approximate solution by picking a reasonable form for $f(\theta)$ containing an unknown constant and determine the constant by evaluating the integral. Before a bit of further analysis to identify reasonable choices, we review our assumptions. Elastic compressibility, rather than our assumed incompressibility, appears unimportant, at least in eq. (32), as only the strain singularity contributes and slip line theory is valid when strains are large compared to initial yield strains. The more serious assumption is that the stress field given by eqs. (27) is assumed to actually occur near the crack tip. As indicated, this stress field is correct if the plastic zone completely surrounds the crack tip. Some as yet unpublished etching experiments by Prof. F. A. McClintock, discussed in [8], reveal a plastic zone that does surround the tip. But other etching experiments [26] are inconclusive on whether yielding actually occurs over any sizable region directly ahead and behind the

crack tip. It is worth noting, however, that the elastic-plastic boundary could cut sharply into the crack tip in regions A and B in fig. 9 without effecting the validity of our stress field very near the tip. In particular, the stresses given by eqs. (27a and b) could be valid right at the crack tip in elastic material, with a steady decay of the resolved shear stress away from the yield value at non-zero distances from the tip in regions A and B . The centered fan could then still result, and eq. (32) remain valid. It is especially interesting that a result of just this sort occurs for the perfectly plastic anti-plane strain crack problem. In that case a construction of the stress field on the assumption of a plastic zone surrounding the tip leads to a fan of anti-plane shear lines centered at the crack tip in the region $x > 0$ of fig. 9 ($\sigma_{\theta z} = \tau_Y$) , and constant stress states adjoining the crack surfaces for $x < 0$ ($\sigma_{xz} = \pm\tau_Y$) . But exact solutions [2,5,7] reveal an elastic-plastic boundary extending ahead of the crack and cutting into the crack tip tangentially to the boundary between the centered fan and constant stress regions. The true plastic zone encloses only points in the centered fan region; in what was apparently a constant stress plastic region, there is elastic behavior with a steady decay of the resolved shear stress away from the yield value as one moves away from the crack tip.

Let us define a function $R(\theta)$ by

$$\gamma_Y R(\theta) = f''(\theta) + f(\theta) \quad . \tag{33a}$$

Then from eqs. (30b,31b), the "engineering" shear strain near the crack tip

in the fan is given by

$$\gamma = \gamma_Y \frac{R(\theta)}{r} \tag{33b}$$

Note from eq. (28b) that this equation would apply throughout the centered fan if $g(r)$ were a linear function of r (as would be the case if the constant state region B in fig. 9 underwent a homogeneous strain). Thus $R(\theta)$ is an approximate indication of the distance to the elastic-plastic boundary, and we can estimate the plastic zone size by writing eq. (32) in the form

$$J = 2\tau_Y \gamma_Y \int_{\pi/4}^{3\pi/4} R(\theta) \left[\cos\theta + \left(1 + \frac{3\pi}{2} - 2\theta\right) \sin\theta\right] d\theta \quad . \tag{33c}$$

For a given choice of $R(\theta)$, displacements near the crack tip are computed from eqs. (30b) by solving the differential equation (33a) under initial conditions $f(\pi/4) = f'(\pi/4) = 0$. It is also useful to write eq. (32) in terms of cartesian components of displacements:

$$\begin{aligned} u_y &= u_r \sin\theta + u_\theta \cos\theta \\ u_x &= u_r \cos\theta - u_\theta \sin\theta \end{aligned} \tag{34a}$$

Differentiating with respect to θ and using eqs. (30b), in the fan

$$\begin{aligned} \frac{du_y}{d\theta} &= [f''(\theta) + f(\theta)] \sin\theta = \gamma_Y R(\theta) \sin\theta \\ \frac{du_x}{d\theta} &= [f''(\theta) + f(\theta)] \cos\theta = \gamma_Y R(\theta) \cos\theta \quad . \end{aligned} \tag{34b}$$

The ordinary differentiation symbol is used as displacements depend only on θ very near the tip. We can then estimate crack opening displacements by writing eq. (32) in the form

$$J = 2\tau_Y \int_{\pi/4}^{3\pi/4} \frac{du_y}{d\theta} \left[\frac{\cos\theta}{\sin\theta} + \left(1 + \frac{3\pi}{2} - 2\theta\right)\right] d\theta \quad . \tag{34c}$$

Let us first consider the crack opening displacement $\delta_t = 2u_y$ at $\theta = 3\pi/4$. Assume as an approximation that $du_y/d\theta$ is symmetric about $\theta = \pi/2$. From eq. (34b), this is equivalent to assuming symmetry of $R(\theta)$ about the vertical: $R(\pi/2 + \beta) = R(\pi/2 - \beta)$. The bracketed term in eq. (34c) may be split into a symmetric part equal to $(1 + \pi/2)$ and an anti-symmetric part. The anti-symmetric contributes zero to the integral and thus

$$J \approx 2\tau_Y (1 + \pi/2) \int_{\pi/4}^{3\pi/4} \frac{du_y}{d\theta} d\theta = (1 + \pi/2)\, \tau_Y \delta_t$$

$$\delta_t \approx \frac{2}{2 + \pi} \frac{J}{\tau_Y} = \frac{2\pi(1 - \nu^2)\sigma_\infty^2 a}{(2 + \pi)\, E\, \tau_Y} \tag{35}$$

Here, as throughout the paper, the latter form applies for small scale yielding near a crack of length $2a$ in a uniform stress field σ_∞. Comparing with the Dugdale plane stress value (eq. 25c) for the same remotely applied stress and crack length, and for $\nu = 0.3$, the plane strain crack opening displacement is 61% of the plane stress value for a Mises yield condition ($\sigma_Y = \sqrt{3}\,\tau_Y$) and 70% for a Tresca yield condition ($\sigma_Y = 2\tau_Y$). Note that if $R(\theta)$ is symmetric about $\theta = \pi/2$, as we have just assumed, then an integration of the latter of eqs. (34b) gives $u_x = 0$ at $\theta = 3\pi/4$. This means that the crack opens up

into a rectangular shaped tip, much as observed by Laird and Smith [26]. An integration by parts in eq. (34c) expresses J in terms of an integral of u_y times a function of θ. From eq. (34b) $du_y/d\theta$ is non-negative since $R(\theta)$ is non-negative, so that $u_y \leq \delta_t/2$. Applying this inequality to the expression for J (after integration by parts), one obtains a lower bound on the crack opening displacement:

$$\delta_t \geq \frac{1}{2+\pi} \frac{J}{\tau_Y} . \tag{36}$$

Our reason for concern with crack opening displacements is shown in fig. 10. The slip line field of fig. 9 suggests no intense strain concentration ahead of the crack. But when the slip line field is drawn for a crack blunted by plastic deformation, a very different picture results on a small scale of the order of δ_t. The fan C becomes non-centered and its straight slip lines focus into a region D of intense deformation. For simplicity of illustration, the crack tip has been drawn as a semi-circle in fig. 10 and the associated exponential spiral slip line field [15,24] extends a distance of $1.9\,\delta_t$ ahead of the blunted tip. From estimates of the plastic zone size to be given shortly, we shall see that δ_t is of the order of the initial yield strain times a linear dimension of the plastic zone, so that the intense deformation region is extremely small and fig. 10 is essentially fig. 9 with a magnification in linear dimensions of the order of one over the initial yield strain. Since the blunted region is small, an effective procedure would be to perform an incremental analysis of blunting by regarding the constant displacement rate along each straight slip line of the noncentered fan to be given by the rate

of increase of $u_r = u_r(\theta)$ of our present analysis (where θ is now the inclination of a given straight slip line and is identical to the polar coordinate θ at distances from the tip large compared to δ_t) .

Calling $R(\theta)$ the distance from the crack tip to the elastic-plastic boundary, as an approximation, let us assume that

$$R(\theta) = R \qquad \text{(a constant)} \tag{37a}$$

so that the boundary is an arc of circle of radius R in the centered fan. Substitution into eq. (33c) estimates the plastic zone dimension as

$$R = \frac{GJ}{\sqrt{2}\,(2+\pi)\,\tau_Y^2} = \frac{\pi(1-\nu)}{2\sqrt{2}\,(2+\pi)} \left(\frac{\sigma_\infty}{\tau_Y}\right)^2 a \tag{37b}$$

We shall see that this is actually the smallest possible value which the maximum value of $R(\theta)$ may have. Near crack tip displacements in the fan associated with this choice of $R(\theta)$ are

$$u_r = \gamma_Y R \sin(\theta - \pi/4)$$

$$u = -\gamma_Y R\,[1 - \cos(\theta - \pi/4)] \tag{37c}$$

Another choice for $R(\theta)$,

$$R(\theta) = R \sin(2\theta - \pi/2) \qquad (R \text{ a constant}) \tag{38a}$$

gives an elastic-plastic boundary which cuts into the crack tip along radial boundaries of the centered fan $(R(\pi/4) = R(3\pi/4) = 0)$ as discussed earlier. In this case eq. (33c) estimates the maximum plastic zone dimension as

$$R = \frac{3GJ}{2\sqrt{2}\,(2+\pi)\,\tau_Y^2} = \frac{3\pi(1-\nu)}{4\sqrt{2}\,(2+\pi)}\left(\frac{\sigma_\infty}{\tau_Y}\right)^2 a \quad , \tag{38b}$$

50% greater than the estimate of eq. (37b) above. Associated near tip displacements are

$$u_r = \frac{2\gamma_Y R}{3}\left[\cos(\theta - \pi/4) - \cos(2\theta - \pi/2)\right]$$

$$u_\theta = -\frac{\gamma_Y R}{3}\left[2\sin(\theta - \pi/4) - \sin(2\theta - \pi/2)\right] \quad . \tag{38c}$$

Comparing with the displacements of eq. (37c), both give the crack opening displacement of eq. (35), as they must since $R(\theta)$ is chosen symmetrical about $\theta = \pi/2$ in both cases. u_r is the input to the large deformation region in an analysis of blunting, and the two predictions of u_r agree identically for $\theta = \pi/4$, $\pi/2$, and $3\pi/4$. The greatest difference occurring for intermediate angles is about 18% of the maximum value of $u_r = \delta_t/(2\sqrt{2})$ occurring at $\theta = 3\pi/4$, so predictions of blunting appear insensitive to the choice of $R(\theta)$.

Comparing the two estimates of plastic zone size (eqs. 37b and 38b) with the plane stress zone size (eq. 26c) predicted by the Dugdale model, for

$\nu = 0.3$ eq. (37b) predicts a plane strain R which is 37% of the plane stress R for a Mises material and 49% for a Tresca material. Corresponding figures for eq. (38b) are 55% and 73% . Observations [27] by etching suggest a figure in the neighborhood of 50% . Eq. (33c) gives a lower bound on the maximum value of $R(\theta)$ occurring in the fan. Inserting the inequality $R(\theta) \leq R_{max}$, one obtains

$$R_{max} \geq \frac{GJ}{\sqrt{2}\,(2+\pi)\,\tau_Y^2} = \frac{\pi(1-\nu)}{2\sqrt{2}\,(2+\pi)} \left(\frac{\sigma_\infty}{\tau_Y}\right)^2 a \quad . \tag{39}$$

The lower bound is identical to the value of R given by eq. (37b) .

References

1. H. B. Phillips, Vector Analysis, John Wiley and Sons, 1959.

2. J. R. Rice, "Stresses Due to a Sharp Notch in a Work Hardening Elastic-Plastic Material Loaded by Longitudinal Shear", to appear in J. Appl. Mech. 1967.

3. B. Budiansky, "A Reassessment of Deformation Theories of Plasticity", Trans. A.S.M.E., vol. 81E (J. Appl. Mech.), 1959.

4. J. R. Rice, "Plastic Yielding at a Crack Tip", Proc. Int'l. Conf. Fracture (1965), Sendai, Japan, 1966.

5. J. R. Rice, "Contained Plastic Deformation Near Cracks and Notches Under Longitudinal Shear", Int'l. J. Fracture Mech., vol. 2, no. 2, June 1966.

6. H. Neuber, "Theory of Stress Concentration for Shear Strained Prismatical Bodies with Arbitrary Non-linear Stress-Strain Law", Trans. A.S.M.E., vol. 83E (J. Appl. Mech.), 1961.

7. G. R. Irwin and M. F. Koskinen, discussion and author's closure to "Elastic-Plastic Deformation of a Single Grooved Flat Plate under Longitudinal Shear", by M. F. Koskinen, Trans. A.S.M.E., vol. 85D (J. Basic Engr.), 1963.

8. J. R. Rice, "The Mechanics of Crack Tip Deformation and Extension by Fatigue", to appear in Symposium on Fatigue Crack Growth (1966), A.S.T.M. Spec. Tech. Publ. 415, 1967.

9. M. L. Williams, "On the Stress Distribution at the Base of a Stationary Crack", Trans. A.S.M.E., vol. 79E (J. Appl. Mech.), 1957.

10. G. R. Irwin, "Fracture Mechanics", in Structural Mechanics (Proc. of First Naval Symp.), Pergamon Press, 1960.

11. N. I. Muskelishvili, Some Basic Problems in the Mathematical Theory of Elasticity, English trans. by J. Radok, P. Noordhoff and Co., 1953.

12. P. C. Paris and G, C. Sih, "Stress Analysis of Cracks", in Symposium on Fracture Toughness Testing and its Applications, A.S.T.M. Spec. Tech. Publ. 381, 1965.

13. J. D. Eshelby, "The Determination of the Elastic Field of an Ellipsoidal Inclusion and Related Problems", Proc. Roy. Soc. A, vol. 241, 1957.

14. S. Timoshenko and J. N. Goodier, Theory of Elasticity, McGraw-Hill, 2nd ed., 1951.

15. R. Hill, The Mathematical Theory of Plasticity, Clarendon Press, Oxford, 1950.

16. A. A. Griffith, "The Phenomena of Rupture and Flow in Solids", Phil. Trans. Royal Soc., London, vol. A221, 1921.

17. J. R. Rice and D. C. Drucker, "Energy Changes in Stressed Bodies due to Void and Crack Growth", to appear in International Journal of Fracture Mechanics, 1967-68.

18. G. I. Barenblatt, "Mathematical Theory of Equilibrium Cracks in Brittle Fracture", in Advances in Applied Mechanics, vol. VII, Academic Press, 1962.

19. D. Dugdale, "Yielding of Steel Sheets Containing Slits", J. Mech. Phys. Solids, vol. 8, 1960.

20. G. T. Hahn and A. R. Rosenfield, "Local Yielding and Extension of a Crack under Plane Stress", Acta Met., vol. 13, no. 3, 1965.

21. A. A. Wells, "Application of Fracture Mechanics at and Beyond General Yielding", British Welding Journal, Nov. 1963.

22. B. A. Bilby and K. H. Swinden, "Representation of Plasticity at Notches by Linear Dislocation Arrays", Proc. Roy. Soc. A, vol. 285, 1965.

23. E. H. Lee, "Plastic Flow in a V-Notched Bar Pulled in Tension", Trans. A.S.M.E., vol. 74E (J. Appl. Mech.), 1952.

24. W. Prager and P. G. Hodge, Jr., Theory of Perfectly Plastic Solids, John Wiley and Sons, 1951.

25. F. A. McClintock, "Effect of Root Radius, Stress, Crack Growth, and Rate on Fracture Instability", Proc. Roy. Soc. A, vol. 285, 1965.

26. C. Laird and G. C. Smith, "Crack Propagation in High Stress Fatigue", Phil. Mag., vol. 7, 1962.

27. G. T. Hahn and A. R. Rosenfield, "Experimental Determination of Plastic Constraint Ahead of a Sharp Crack Under Plane Strain Conditions", Ship Structure Committee Report, SSC-180, Dec. 1966.

dwa

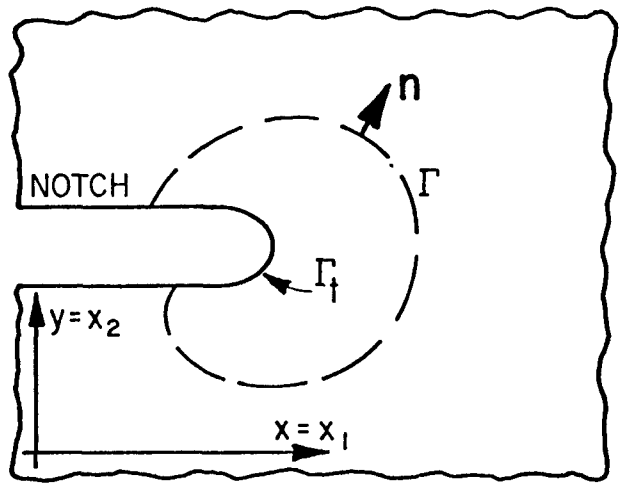

fig. 1. Flat surfaced notch in two-dimensional deformation field (all stresses depend only on x and y). Γ is any curve surrounding the notch tip; Γ_t denotes the curved notch tip.

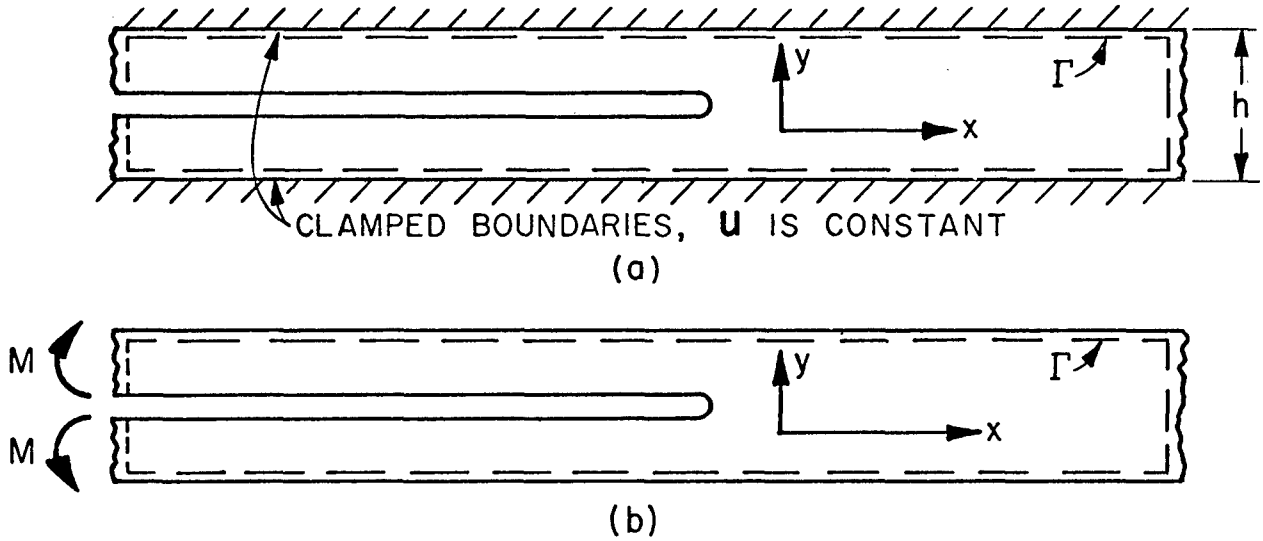

fig. 2. Two special configurations for which the path independent integral J is readily evaluated on the dashed line paths Γ shown. Infinite strips with semi-infinite notches, (a) constant displacements imposed by clamping boundaries, and (b) pure bending of beam-like arms.

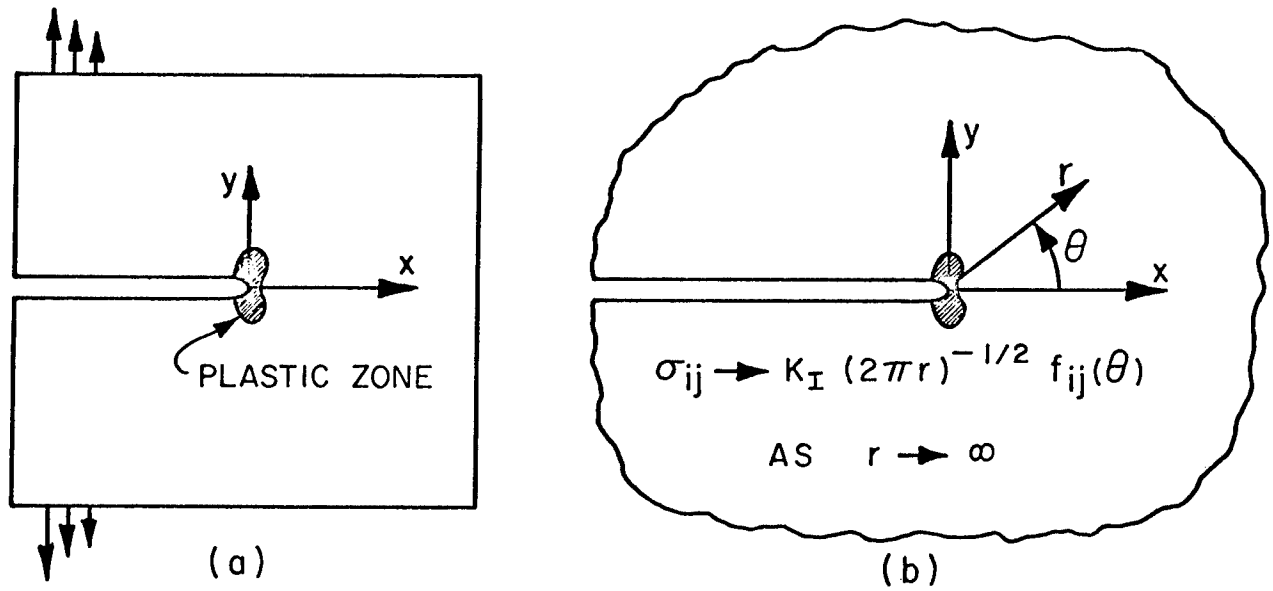

fig. 3. (a) Small scale yielding near a narrow notch or crack in an elastic-plastic material. (b) The actual configuration is replaced by a semi-infinite notch or crack in an infinite body, actual boundary conditions are replaced by the requirement of an asymptotic approach to the linear elastic crack tip singularity stress field.

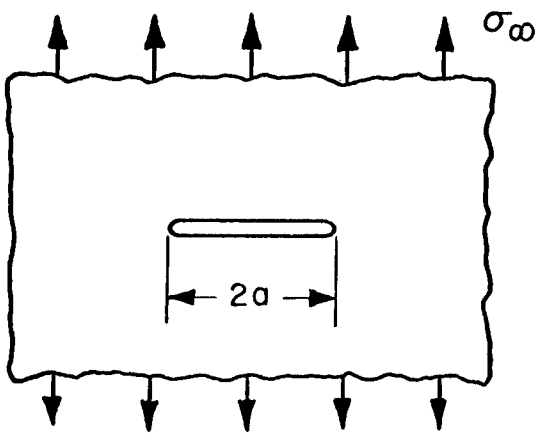

fig. 4. Narrow notch or crack of length 2a in infinite body. Uniform remote stress σ_∞ .

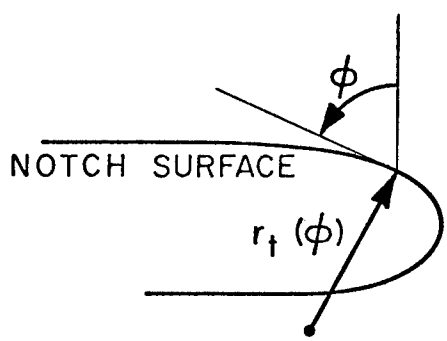

fig. 5. Coordinates employed in description of notch surface. ϕ is tangent angle and $r_t(\phi)$ is radius of curvature.

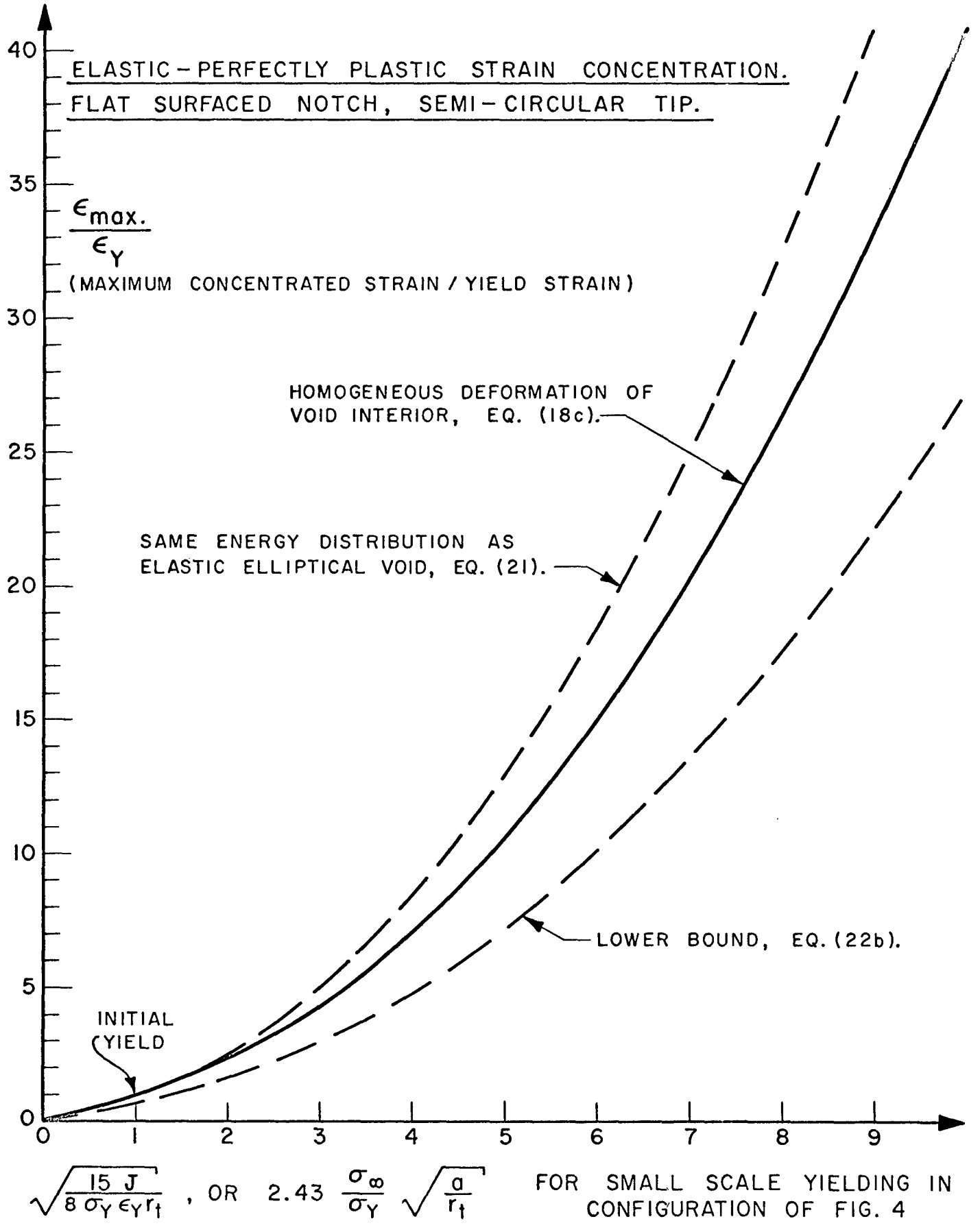

fig. 6. Strain concentration by flat surfaced notch with semi-circular tip of radius r_t in perfectly plastic material.

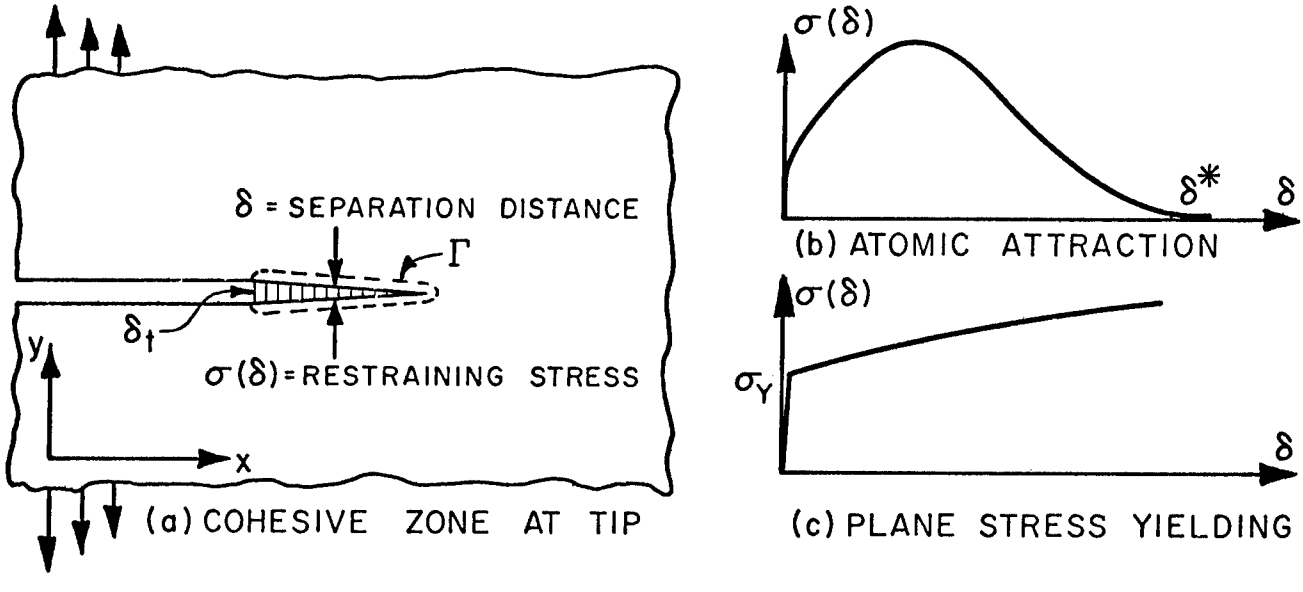

fig. 7. Dugdale-Barenblatt crack model. (a) Cohesive zone at crack tip with restraining stress dependent on separation distance. (b) Force-displacement relation for atomic attraction in elastic brittle fracture, and (c) for plane stress plastic yielding in thin sheet.

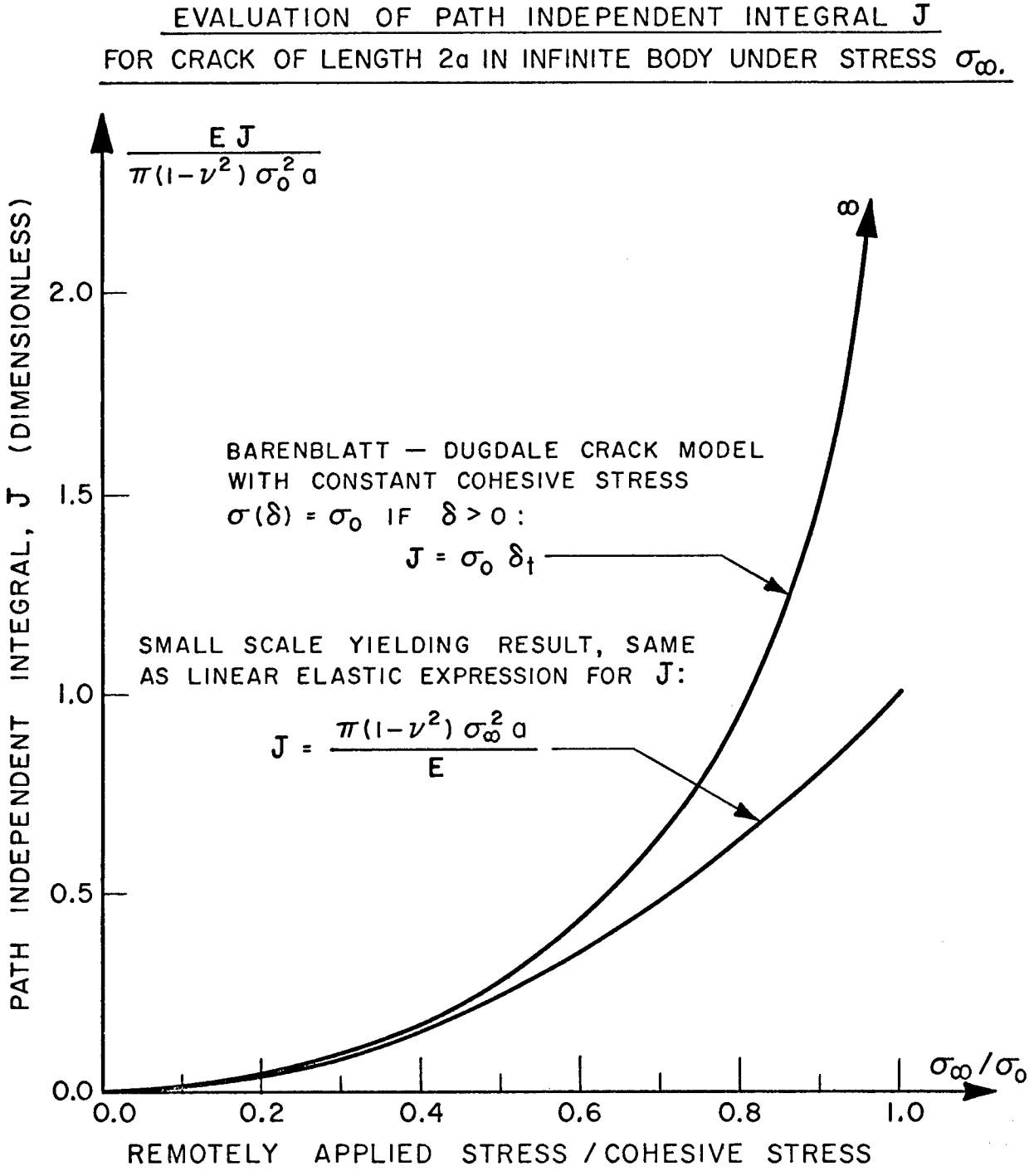

fig. 8. Comparison of small scale yielding result for J with exact value from Barenblatt - Dugdale crack model (can be used to approximate J in the large scale yielding range for other problems of cracks or narrow notches).

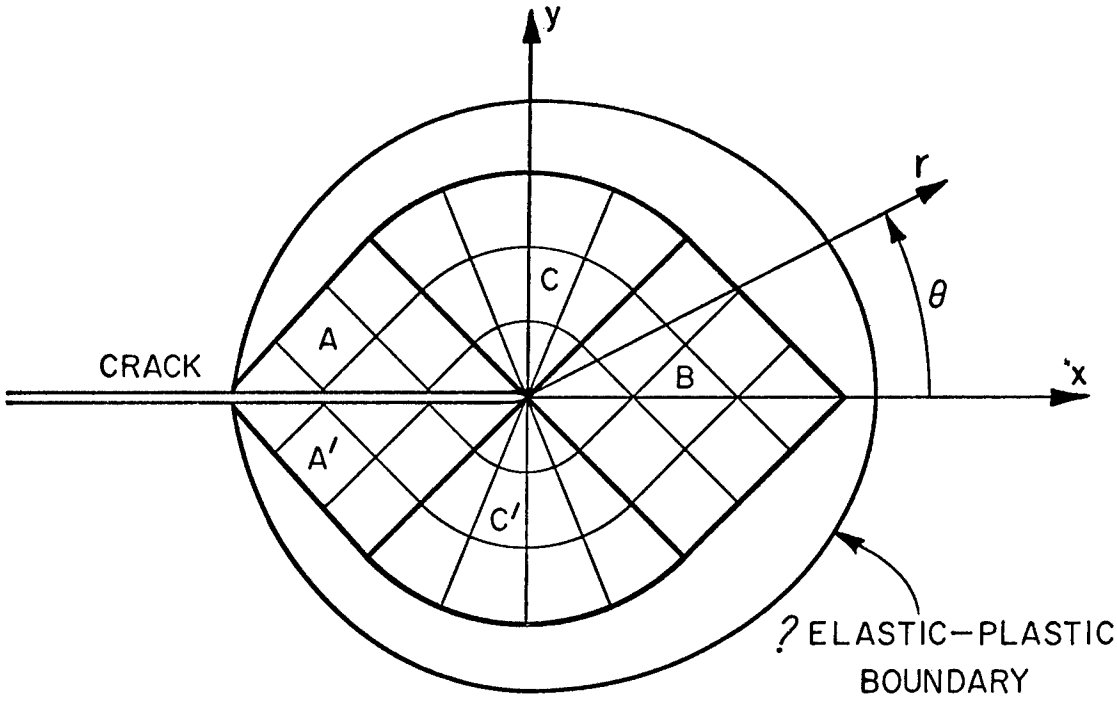

fig. 9. Perfectly plastic plane strain slip line field at a crack tip. Constant stress regions A and B joined by centered fan C . Position of the elastic-plastic boundary is unknown; it may cut in toward the crack tip in regions A and B (see discussion).

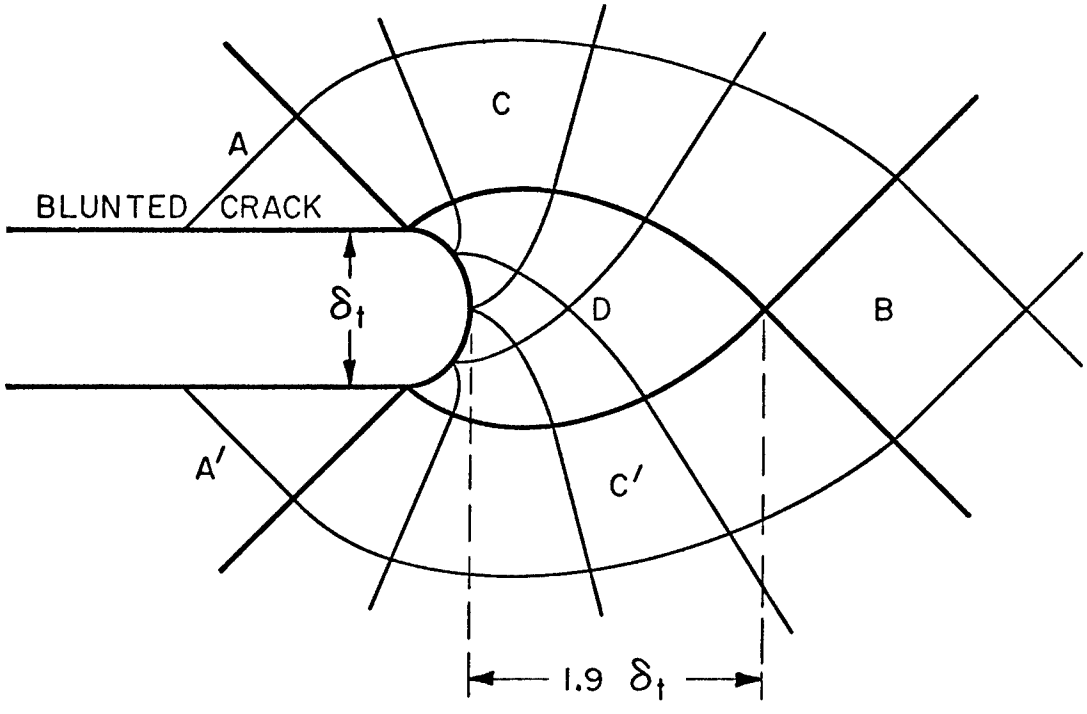

fig. 10. Crack tip blunting creates a small region D of intense deformation ahead of the crack. This is fig. 9 magnified in linear dimensions by a large factor of the order of one over the initial yield strain.